Remote Sensing of Environment 165 (2015) 1–13

Contents lists available at ScienceDirect

Remote Sensing of Environment

journal homepage: www.elsevier.com/locate/rse

Reconstructing hydrographic change in Petersen Bay, Ellesmere Island, Canada, inferred from SAR imagery

Adrienne White [a], Derek Mueller [b], Luke Copland [a]

[a] Department of Geography, University of Ottawa, 60 University Pvt., Ottawa, Ontario K1N 6N5, Canada
[b] Department of Geography and Environmental Studies, Carleton University, B349 Loeb Building, 1125 Colonel By Drive, Ottawa, Ontario K1S 5B6, Canada

ARTICLE INFO

Article history:
Received 21 July 2014
Received in revised form 17 April 2015
Accepted 21 April 2015
Available online xxxx

Keywords:
Ice-dammed lake
Ice shelf
Sea ice
Epishelf lake
Synthetic aperture radar
Arctic

ABSTRACT

Synthetic aperture radar (SAR) satellite imagery was used to reconstruct the change in limnological conditions adjacent to an Arctic ice shelf by examining the backscatter values of coastal ice in mid-winter scenes. High SAR backscatter values (>−6 dB) suggest that an ice-dammed lake was present adjacent to the south coast of Petersen Bay from 1992 until 2005. Following a large calving event of the adjacent Petersen Ice Shelf (−8.07 km^2) in August 2005, the lake drained through a region where the ice shelf had separated from the coastline. This loss of freshwater and replacement of lake ice with sea ice along the southern coast of Petersen Bay were confirmed from analyses of ice core samples and conductivity–temperature–depth (CTD) profiles. The exception to this pattern was one distinct area where terrestrial streams entered the edge of Petersen Bay and freshwater continued to collect from 2006 to 2008. However, this ephemeral area of freshwater has not reformed since 2009 due to the persistence of open water events in Petersen Bay (observed in optical satellite imagery), which likely facilitated mixing of freshwater with sea water. Based on the continued break-ups of Petersen Ice Shelf and the frequency of open water events, it is unlikely that this ice-dammed lake will reform. The results of this study underscore the utility of SAR for reconstructing past hydrographic conditions in the water column below.

1. Introduction

The Arctic is currently in a period of transformation due to climate change. Since the 1950s, annual pan-Arctic (60–90°N) surface air temperatures have increased by >2 °C, and the period 1999–2008 was the warmest over the past 2000 years (AMAP, 2011; Kaufman et al., 2009). The impacts on the cryosphere of this warming are readily monitored using remote sensing. For example, laser and radar altimetry, along with satellite-derived gravity measurements, have detected mass wasting of ice sheets, ice caps and glaciers (e.g., Gardner et al., 2011; Shepherd et al., 2012). Passive microwave and laser altimeter data have revealed declines in Arctic seasonal and multiyear sea ice (MYI) extent, with concomitant reductions in age and thickness (Comiso, Parkinson, Gersten, & Stock, 2008; Kwok & Rothrock, 2009; Maslanik, Stroeve, Fowler, & Emery, 2011; Stroeve, Holland, Meier, Scambos, & Serreze, 2007). The resulting increase in open water conditions along the northern coast of Ellesmere Island at the northern limit of North America, in combination with warmer temperatures and high winds, has been associated with the dramatic loss of ice shelves (Copland, Mueller, & Weir, 2007; White, Copland, Mueller, & Van Wychen, 2015). The ice shelves in this region comprise thick masses (>20 m) of floating landfast sea ice and glacier ice that formed up to 5500 years before present, and had an estimated area of ~9000 km^2 at the start of the 20th century (England et al., 2008; Jeffries, 1992b; Vincent, Gibson, & Jeffries, 2001). Over the last century they have lost >90% in areal extent, with an additional ~40% loss since 2005 (Mueller, Crawford, Copland, & Van Wychen, 2013; Mueller, Vincent, & Jeffries, 2006).

Studies are limited about the impacts of Arctic ice shelf losses on the surrounding environment, particularly on ice-dammed lakes, a unique type of lake that is structurally dependent on the presence of coastal ice (e.g. Mueller, Vincent, & Jeffries, 2003). An ice-dammed lake forms where a layer of relatively low density freshwater, underlain by higher density marine water, becomes impounded at the head of fiords and embayments behind an ice shelf (Fig. 1; Jungblut, Mueller, & Vincent, In press; Veillette, Mueller, Antoniades, & Vincent, 2008; Veillette et al., 2011). The freshwater that collects behind the dam typically originates from summer meltwater inflow from the surrounding catchment and will accumulate to form a layer that is as deep as the minimum draft of the ice that blocks the fiord or bay (Keys, 1977). A perennial ice cover on the lake surface prevents mixing by winds, thus allowing the freshwater layer to remain permanently stratified over the marine water below (Veillette et al., 2008). There are two types of ice-dammed lakes: shallow ice-dammed lakes that are dammed by relatively thin

E-mail addresses: awhit059@uottawa.ca (A. White), derek.mueller@carleton.ca (D. Mueller), luke.copland@uottawa.ca (L. Copland).

http://dx.doi.org/10.1016/j.rse.2015.04.017
0034-4257/

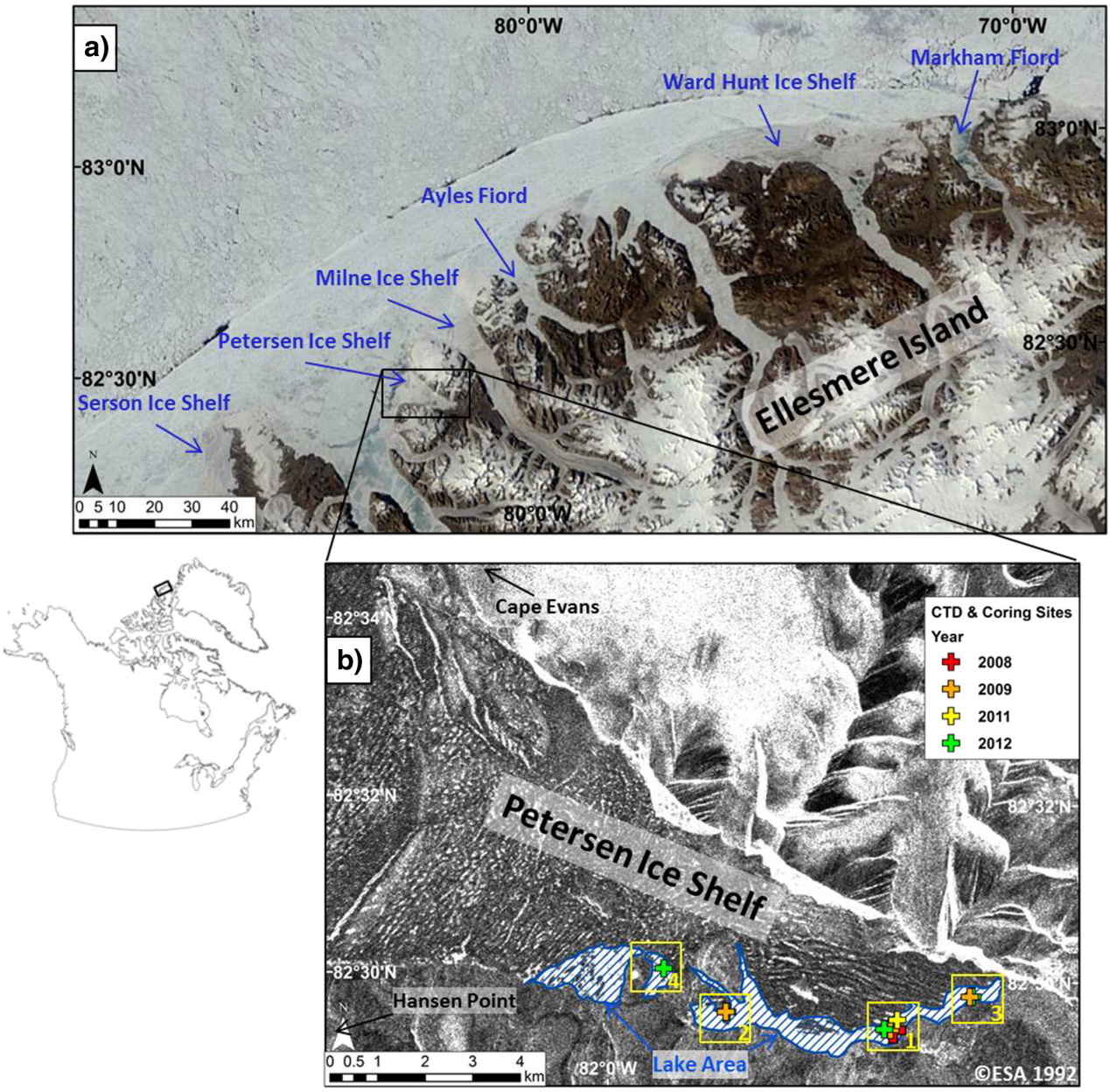

Fig. 1. (a) MODIS image (August 1, 2011) showing the location of the remaining ice shelves as of summer 2011, and inset map showing location of the northern coast of Ellesmere Island; (b) Annotated ERS-1 Standard (VV) scene from March 16, 1992, denoting the location of each CTD (Conductivity–temperature–depth) and ice coring site across the Petersen Bay study area. The striped area represents the extent of the ice-dammed lake in Petersen Bay. Yellow boxes denote the study areas for ice core and CTD measurements. No ice core was extracted in 2008. (For interpretation of the references to color in this figure legend, the reader is referred to the web version of this article.)

multiyear landfast sea ice (MLSI) and have a freshwater layer <5 m deep (Jeffries, 1992a; Jungblut et al., in press; Veillette et al., 2008), and epishelf lakes, an ice-dammed lake that is blocked by an ice shelf forming a freshwater layer that is thicker than 5 m.

The existence of an ice-dammed lake is strongly dependent upon the thickness and structure of its adjacent ice dam, meaning that changes in the dam thickness can result in a thinning of the freshwater layer. If the structural integrity of an ice dam is compromised (e.g., due to fracturing or calving), the lake can be lost entirely. For example, the epishelf lake in Disraeli Fiord drained away completely when the Ward Hunt Ice Shelf fractured in the early 2000s (Mueller et al., 2003). Leading up to this drainage event, the Ward Hunt Ice Shelf had thinned by 13 m (27%) between 1967 and 1999 (Vincent et al., 2001). Between 2000 and 2002 vertical fracturing occurred all the way through the ice shelf, providing a conduit through which the freshwater drained (Mueller et al., 2003). As a result of this drainage event, both the epishelf lake and the unique biota found within it were lost.

Recent studies have highlighted the importance of ice-dammed lakes as unique habitats for microbial ecosystems due to their vertical segregation between layers of fresh, brackish and marine water (Veillette et al., 2011). For example, the Milne Fiord epishelf lake provides a habitat for diverse microbial communities of Eukarya, Eubacteria, Archaea, and viruses, and epishelf lakes in both the Arctic and Antarctic also offer a unique habitat for fresh and brackish water species of zooplankton (Laybourne-Parry, Quayle, Henshaw, Ruddell, & Marchants, 2001; Van Hove, Swadling, Gibson, Belzile, & Vincent, 2001; Veillette et al., 2011).

Ice-dammed lakes were first characterized by measuring salinity throughout the water column to detect the marked change in water properties with depth (Crary, 1960; Heywood, 1977; Keys, 1977). Due

to logistical constraints, in situ measurements have been limited and continue to be difficult to obtain with enough spatial and temporal variability to examine the vast remote areas of the Polar Regions. However, in recent years, Jeffries (2002) and Jeffries, Morris, and Kozlenko (2005) noted that SAR satellite imagery could be useful for identifying ice-dammed lakes due to the high backscatter response in mid-winter imagery. Veillette et al. (2008) exploited this observation, along with in situ salinity and temperature profiles, to examine the distribution of ice-dammed lakes across northern Ellesmere Island using winter Radarsat-1 SAR scenes from 2005, 2006 and 2007. Their analysis suggests that the perennial ice cover of these ice-dammed lakes have backscatter levels that typically exceeded −6.0 dB, while surrounding sea ice and ice shelf ice had a lower backscatter. By applying this threshold to the SAR scenes, they concluded that nine ice-dammed lakes were present across this coastline in 2008, along with one deep epishelf lake that remained behind the Milne Ice Shelf at this time. The Veillette et al. (2008) assessment did not identify an ice-dammed lake in Petersen Bay, although Mueller et al. (2006) suggest that one was probably present in 2000 from an analysis of SAR data. However, no previous in situ measurements had been made there to confirm this.

The first objective of this study is to test the use of a SAR backscatter threshold to distinguish perennial lake ice from other ice types and infer the presence or absence of an ice-dammed lake. The second objective is to use this method, along with ancillary remote sensing data and in situ observations, to reconstruct changes in the physical oceanography/limnology of Petersen Bay and interpret these in the context of cryospheric change on the Petersen Ice Shelf. Our approach makes use of SAR scenes from 1992 to 2012, optical scenes from 2002 to 2012, as well as ice cores and CTD (conductivity–temperature–depth) profiles collected since 2008.

2. Study area

Petersen Bay is located on the northern coast of Ellesmere Island, Nunavut, to the southwest of the Milne Ice Shelf between Hansen Point and Cape Evans (Fig. 1). This bay contains the Petersen Ice Shelf (unofficial name; 82°31′N, 81°56′W), which is currently only connected to the northern coast of the bay. The area between the ice shelf and southern coastline contains the area where an ice-dammed lake would have been expected (prior to 2012, when the ice shelf extended to the southern coast), and is the area under investigation in this study (Fig. 1b). According to observations based on an interpretation of SAR satellite data from 2000, Mueller et al. (2006) reported that the Petersen Ice Shelf had a length of 17 km and width of 12 km, with >100 km^2 of MLSI at its front and an epishelf lake area of 7.3 km^2. In the study of White et al. (2015), a combination of aerial photography, and optical and SAR satellite imagery were used to determine that the Petersen Ice Shelf was stable until June 2005, after which break-up began to occur. Calving events from the ice shelf in 2005, 2008, 2011 and 2012 resulted in a 61% loss of the 2005 area. As of August 2012, the total surface area of the ice shelf was 19.32 km^2, with a mean ice thickness of ~29 m (White et al., 2015).

3. Methods

3.1. SAR backscatter analysis

An analysis of backscatter patterns in SAR imagery is used to determine if the ice cover connected to the ice shelf in Petersen Bay is currently, or was previously, perennial freshwater ice. This is then used to infer the presence or absence of an ice-dammed lake. Backscatter analysis provides an effective method for distinguishing floating lake ice during periods of sub-freezing air temperatures (i.e., winter, spring), due to the lack of liquid brine resulting in negligible absorption of the radar signal and a strong reflection at the ice–water interface due to the strong dielectric contrast. As well, perennial freshwater ice in this region, from adjacent Milne Fiord, contains vertically-oriented bubbles (ranging from ~1–12 cm long) and large vertically-oriented crystals (up to 12.5 cm; M. Richer-McCallum, unpublished). These vertical elements and the horizontal ice–water interface are thought to cause a double-bounce reflection which returns the incident energy to the sensor at a similar angle to when it was originally transmitted, resulting in high backscatter values (Jeffries, Morris, Weeks, & Wakabayashi, 1994). In contrast, sea ice has a relatively low backscatter, caused primarily by the absorption of the radar signal in liquid brine/saline ice. On young and FYI, surface scattering processes are dominant, while volume scattering increases as sea ice ages due to desalination and increased surface roughness (Johnston & Timco, 2008). Volume scattering is also facilitated by the presence of bubbles around the same size as the SAR wavelength (e.g. 5.6 cm for C-Band) (Onstott & Shuchman, 2004).

To complete this analysis, winter and spring (January to May) ERS-1, Radarsat-1, and Radarsat-2 SAR images were used to avoid any influence from surface melt (Table 1). The ERS-1 and Radarsat-1 data were provided by the Alaska Satellite Facility (ASF), and the Radarsat-2 data were acquired through the Canadian Space Agency's Science and Operational Applications Research-Education (SOAR-E) program. The satellite data were radiometrically-corrected to a normalized radar cross-section (σ^0) in a linear power scale to standardize the images. MapReady software version 3.0.6, provided by ASF (http://www.asf.alaska.edu/downloads/software_tools), was used to produce the corrected Radarsat-1 and ERS-1 data using the following equation:

$$\sigma^0 = 10 \times \log\left(a^2\left(\mathrm{DN}^2 - a^1 \times n(r)\right)\right) \quad (1)$$

where DN is the digital number, a^1 and a^2 are the noise scaling and linear conversions and $n(r)$ is noise as a function of range. For the Radarsat-2 data, a look-up table is included with the product which allows the conversion to σ^0:

$$\sigma^0 = (\mathrm{DN})^2/\mathrm{A}^2 \quad (2)$$

where DN is the digital number (0–65,535) and A is the gain value corresponding to the along-range sample. A low pass 3 × 3 averaging filter was applied over each raster cell for every satellite scene to smooth the image and minimize speckle. The statistics reported here were calculated using σ^0 values in a linear power scale followed by conversion to a logarithmic scale (dB).

Veillette et al. (2008) determined that freshwater lakes typically had a return of >−6.0 dB in Radarsat-1 scenes, while sea ice and ice shelf ice had much lower values. To test if this threshold would be appropriate in the current study, a transect of values across the lake ice, ice shelf, and sea ice was extracted from a Radarsat-1 fine beam image from February 14, 2008 (Fig. 2). This was the closest available scene to an April 2008 CTD profile (at site 1 in Fig. 1b) which recorded the presence of lake ice and underlying freshwater. The backscatter across each ice type was compared to the threshold presented by Veillette et al. (2008) and Jeffries et al. (1994); Fig. 2 inset. The mean returns are −4.2 dB for lake ice, −12.5 dB for the ice shelf and −19.8 dB for the first year sea ice in this scene. The low return for sea ice is caused by its relatively high salinity, while the ice shelf has a stronger return due its lower salinity (Jeffries & Sackinger, 1990). Based on the differences between the returns of each ice type, the −6 dB value was determined as a suitable threshold to delineate ice-dammed lake ice from other ice types.

To further validate the choice of −6 dB and evaluate the variability between SAR scenes (including effects such as varying sensors, beam modes, orbit direction and incidence angles), the returns along the sampling transect (Fig. 2) were extracted for every image used in the backscatter analysis (shown in bold in Table 1; Fig. 3). All images prior to the first major calving event of the Petersen Ice Shelf (1992–2005; Fig. 3a) were compared separately from all images after the break-up event (when it was anticipated that the shallow ice-dammed lake had drained) (2006–2012; Fig. 3b). Prior to 2006, the range in backscatter

Table 1
Aerial photography and satellite imagery used in this study. Dates shown in bold were used in the backscatter analysis.

Sensor(polarization)	Date, time (YYYY–MM–DD, HH:MM:SS)	Mid-scene incidence angle (°)	Incidence angle range for the Petersen Ice Shelf (°)	Orbit(descending or ascending)	Pixel size(m)
Aerial photographs A16724-63 & A16724-64	1959-08-13	–	–	–	6.6
ERS-1 Standard (VV)	**1992-03-16, 00:44:40**	23.1	24.2–24.9	Ascending	12.5
	1993-05-19, 00:28:03	23.0	21.8–22.4	Ascending	12.5
	1994-05-18, 00:44:40	23.0	24.3–25.0	Ascending	12.5
	1995-02-24, 00:41:19	23.0	23.7–24.4	Ascending	12.5
Radarsat-1 Standard (HH)	1998-04-16, 22:15:02	46.8	44.8–45.4	Ascending	12.5
	2005-03-18, 19:58:56	22.5	22.2–22.8	Ascending	12.5
	2005-08-18, 22:16:32	46.7	45.6–46.1	Ascending	12.5
	2005-08-23, 19:50:16	22.5	21.0–21.4	Ascending	12.5
	2006-01-14, 19:50:16	22.5	21.0–21.4	Ascending	12.5
Radarsat-1 ScanSAR Wide B (HH)	**1997-02-11, 20:46:59**	34.6	29.9–30.5	Ascending	50
	1998-02-06, 20:47:12	34.6	29.9–30.5	Ascending	50
	1999-01-08, 20:47:17	34.6	29.8–30.5	Ascending	50
	2000-02-02, 21:11:56	34.5	34.2–34.9	Ascending	50
	2001-01-06, 13:04:04	34.7	41.0–41.8	Descending	50
	2002-02-06, 20:34:05	34.5	27.6–28.3	Ascending	50
	2003-01-11, 20:46:03	34.6	29.8–30.5	Ascending	50
	2004-12-07, 20:45:02	34.5	29.8–30.5	Ascending	50
Radarsat-1 Fine (HH)	**2007-01-26, 21:34:02**	38.0	38.7–39.2	Ascending	6.25
	2008-02-14, 21:34:03	38.0	38.7–39.2	Ascending	6.25
Radarsat-2 Wide (HH)	**2009-02-02, 22:02:39**	42.0	43.0–43.5	Ascending	12.5
	2010-03-03, 13:51:07	35.1	33.0–33.8	Descending	12.5
Radarsat-2 Ultrafine (HH)	**2011-04-01, 20:39:32**	28.6	28.3–29.1	Ascending	2.23
Radarsat-2 Ultrafine Wide (HH)	2012-02-03, 20:56:19	32.1	31.3–32.0	Ascending	2.4
	2012-03-22, 20:56:20	32.1	31.3–32.0	Ascending	2.4
ASTER Level 1B	2002-08-14,2003-07-03 2005-03-06, 2005-08-18 2005-08-23, 2006-07-24, 2007-07-14, 2008-08-22 2009-07-16, 2009-07-21 2010-07-02, 2010-07-19 2012-07-15	–	–	–	15

values across each ice type reveals that sea ice returns were consistently more than one standard deviation below −6 dB, while lake ice returns remained above −6 dB. The mean ice shelf returns remained below the −6 dB threshold for both periods, although backscatter values at one standard deviation were above this threshold. These higher returns likely result from the freshwater meltponds that occur in the troughs between the ridges on the ice shelf surface.

After the first major calving from the Petersen Ice Shelf, the returns along the sampling transect (Fig. 2) changed across all the post-2005 SAR scenes. The first 6.5 km (from west to east) of the transect show a cluster of returns below the −6 dB threshold, consistent with sea ice (Fig. 3b). Next, the section of the transect with coverage over the ice shelf had shrunk by ~2 km due to loss of the ice shelf since 2005, and all scenes in this region had a range of backscatter with a mean below the −6 dB threshold, with locally higher returns consistent with the signature of freshwater meltponds on the ice shelf surface (Fig. 3b). At the eastern end of the transect, the region that had lake ice coverage prior to 2006 revealed returns consistent with sea ice for all scenes from 2006–2012 (Fig. 3). The slightly lower sea ice backscatter values in this area compared to those at the western end of the transect are likely due to the development of smoother FYI that formed in this protected area at the back of Petersen Bay. Based on the results of this analysis, it is clear that the sigma nought values extracted from the SAR imagery varied little due to differences in image acquisition characteristics (e.g., orbit, incidence angle, time of year), but did vary greatly based on ice conditions across Petersen Bay. This provides confidence in the use of a −6 dB threshold to identify lake ice in this study.

To further evaluate the −6 dB threshold, an accuracy assessment was used to evaluate the relationship between the reference data ('ground truth') and the corresponding results of the threshold classification on SAR imagery (Lillesand, Kiefer, & Chipman, 2008). An error matrix was produced for each image type used in the backscatter analysis to calculate:

(a) Overall accuracy: the total number of correctly classified pixels divided by the total number of reference pixels;
(b) Producer's accuracy: the number of correctly classified pixels for each ice type divided by the total number of reference pixels used for each category, which determines how well reference pixels identified an ice type;
(c) User's accuracy: the number of correctly classified pixels for each ice type divided by the total number of pixels that were classified for that particular ice type, which represents commission error and how likely a pixel classified as a given ice type is actually that ice type in reality (Lillesand et al., 2008).

The Kappa coefficient was also calculated to evaluate how likely a correct classification was due to chance or due to correct classification (Lillesand et al., 2008). Based on the results of the accuracy assessment there is minimal error associated with the threshold selected (−6 dB), and the difference between sensors indicates that the classification is slightly improved in images with a higher resolution (Table 2).

To determine if changes in ice type were spatially uniform along the entire bay, six sites were examined across the southern margin of Petersen Bay where high backscatter had been detected in 1992 (A–F; Fig. 4). A 260 × 260 m (0.07 km^2) square polygon was used to extract a mean backscatter at each of these sites over each year in the study.

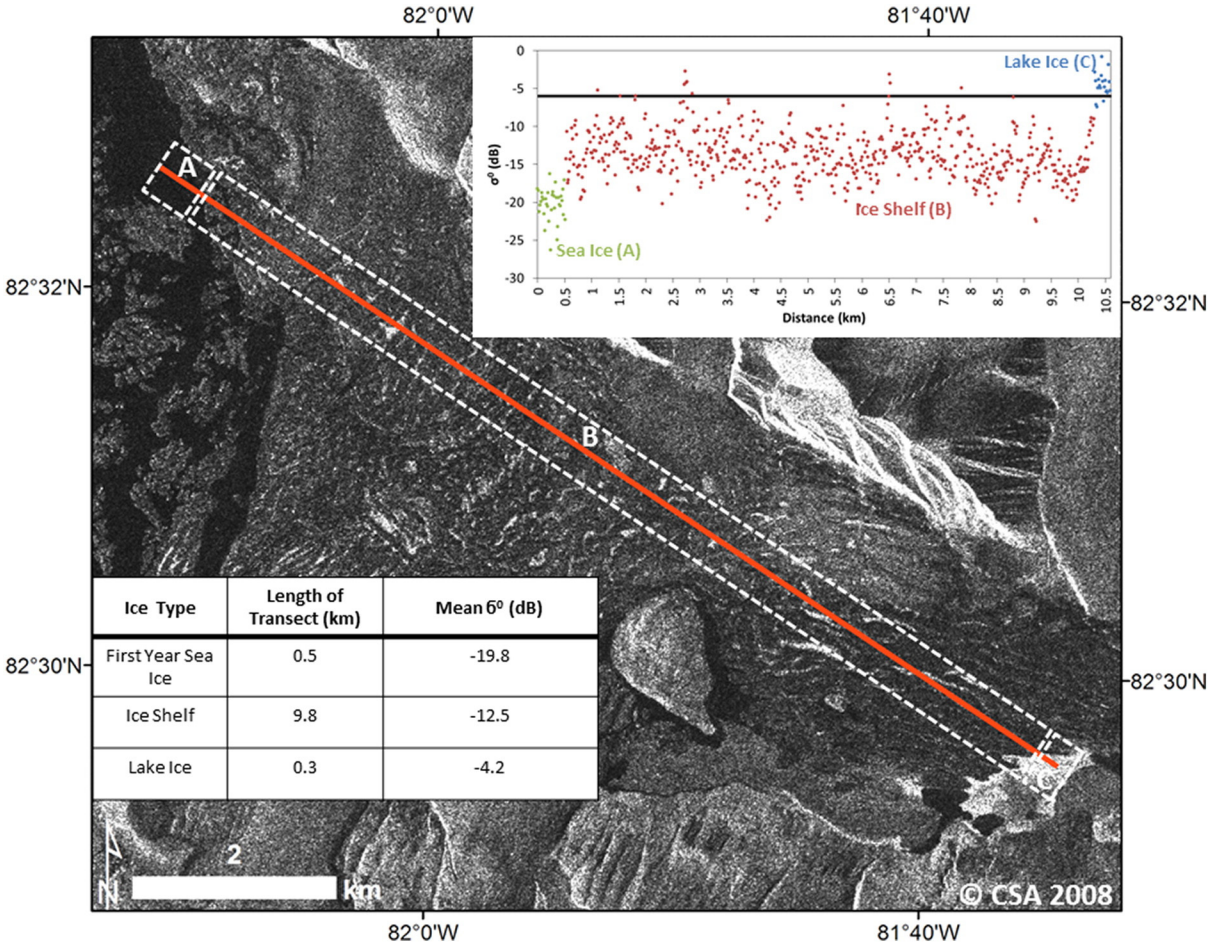

Fig. 2. Radarsat-1 fine scene (Feb. 14, 2008) showing the 10.6 km transect (in red) used to extract sigma nought values from different ice types shown in the inset graph: (A) first year sea ice, (B) ice shelf, (C) lake ice. The solid line in the scatterplot represents the −6 dB threshold chosen to delineate lake ice from other ice types. Inset table: transect length and mean sigma nought value for each ice type. (For interpretation of the references to color in this figure legend, the reader is referred to the web version of this article.)

3.2. Field measurements

Field measurements were completed in Petersen Bay in spring (April/May) 2008, 2009, 2011 and 2012 to support the SAR data interpretation. CTD profiles were obtained and ice cores were extracted across Petersen Bay at four different sites (Fig. 1b). Site 1 is located towards the east side of the ice shelf along its southern flank. Site 2 was selected to examine changes adjacent to an island that was surrounded by the ice shelf on three sides. Site 3 is located at the very head of the bay near an inflowing stream. Site 4 was selected to examine the area to the west of the island, towards the outlet of the bay.

A Kovacs Mark II ice coring system (internal diameter 8.8 cm) was used to drill the cores, after which a Kovacs ice thickness gauge was lowered into the borehole to measure the ice thickness. The ice cores were laid out in a sled and photographed. An ice saw was then used to slice the core into ~10 cm sections. Within 24 h of extraction, the cores were visually assessed for color, cloudiness (whether the ice was clear or opaque), and bubble inclusions. The specific conductivity of the meltwater was measured using a YSI Pro Plus multiparameter probe in 2012, an EC meter model 2052 in 2011, an Oakton PCS Testr 35 in 2009 and an XR-420-CTDm (RBR Global Ltd.) in 2008. Each of these instruments was calibrated against conductivity standards prior to use. Conductivity was converted to salinity using the calculation by Fofonoff and Millard (1983).

An RBR XR-420-CTDm (in 2008) or XR-620-CTDm (in 2009, 2011 and 2012) profiler was lowered through the water column beneath each borehole to determine the conductivity and temperature with depth. Before lowering the profiler, the probe was left in the water to equilibrate for at least 1 min. The measurements sampled at 1 Hz (in 2008) or 6 Hz (2009, 2011, 2012) on the downcast were used in this study. Upcast data were not used to avoid measurements influenced by turbulence created by the CTD housing. Conductivity was converted to salinity using the same method outlined above.

3.3. Analysis of aerial photography and optical satellite imagery

To place environmental changes in Petersen Bay into a larger context, aerial photography and optical satellite imagery were used to monitor related changes to the Petersen Ice Shelf, including the presence of sea ice at the front of the ice shelf, the occurrence of open water events along the southern edge of the ice shelf, and the calving of tributary glaciers into the bay (Fig. 5a). The ice shelf is easily distinguished from adjacent sea ice due to its characteristic rolling surface topography (Fig. 5a), compared to the southern portion of Petersen Bay which contains smooth ice characteristic of lake ice or young sea ice. Vertical aerial photographs were obtained from the National Air Photo Library (Ottawa, Ontario) in TIFF format at a resolution of 1200 dpi (Table 1). Two photographs from August 1959 were cropped and mosaicked. The mosaicked photograph was georeferenced using a first-order polynomial transformation to a cloud-free ASTER L1B scene (July 16, 2009) that was used as the master image against which all other imagery was aligned. A total of 10 ground control points (GCPs)

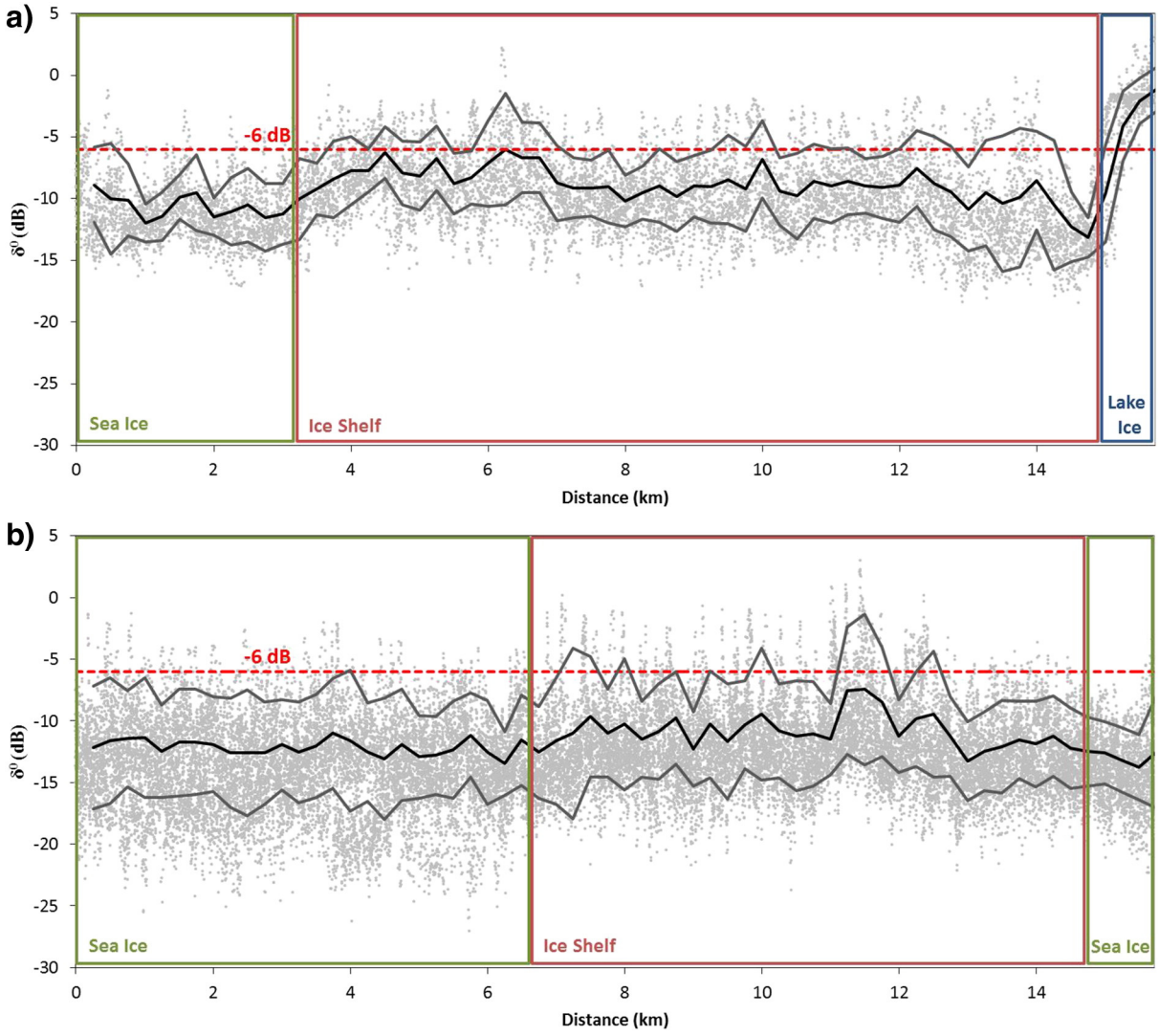

Fig. 3. Sigma nought values extracted from the transect (shown in Fig. 2) for all SAR imagery used in the study from: (a) 1992 to 2005 and (b) 2005 to 2012. The solid black line represents the running average (every 250 m) and the solid gray lines represent +/− one standard deviation. Note: the boundary between ice shelf and lake ice varies between years due to the changes in ice shelf area.

in stable land areas were used for this process, and the final root mean square error (RMSE) for the georeferenced aerial photo mosaic was 33.25 m. A total of 13 ASTER L1B images were used in this study. These images were well aligned to the July 16, 2009 master image, with only the image from July 3, 2003 requiring additional georeferencing (using 13 GCPs and a final RMSE of 14.93 m).

4. Results

4.1. Temporal lake area change

Extensive areas of very high backscatter were observed along the southern coast of Petersen Bay between 1992 and 2004, which were

Table 2
Accuracy of the classification method for each satellite/beam mode combination used in this study to distinguish between lake ice and other ice types (i.e., ice shelf and sea ice).

Date (YYYY–MM–DD)	Satellite/mode (polarization)	Pixel size (m)	Producer's accuracy (%)		User's accuracy (%)		Kappa coefficient	Overall accuracy
			Lake ice	Other	Lake ice	Other		
1992-03-16	ERS-1 Standard (VV)	12.5	100	90.0	90.9	100	0.90	0.95
1997-02-11	Radarsat-1 ScanSAR Wide B (HH)	50	100	95.0	95.2	100	0.95	0.98
2006-01-14	Radarsat-1 Standard (HH)	12.5	100	95.0	95.2	100	0.95	0.98
2007-01-26	Radarsat-1 Fine (HH)	6.25	100	100	100	100	1	1
2009-02-02	Radarsat-2 Wide (HH)	12.5	100	100	100	100	1	1
2011-04-01	Radarsat-2 Ultrafine (HH)	2.23	100	100	100	100	1	1
2012-03-22	Radarsat-2 Ultrafine Wide (HH)	2.40	100	100	100	100	1	1

To identify the presence of lake ice, a polygon delineating Petersen Bay was first traced in each satellite SAR scene (1992 to 2012) using ESRI ArcMap 9.3.1. All pixels within the polygon above the −6 dB threshold were counted, and this was multiplied by the pixel size to calculate the ice-dammed lake area in each satellite image.

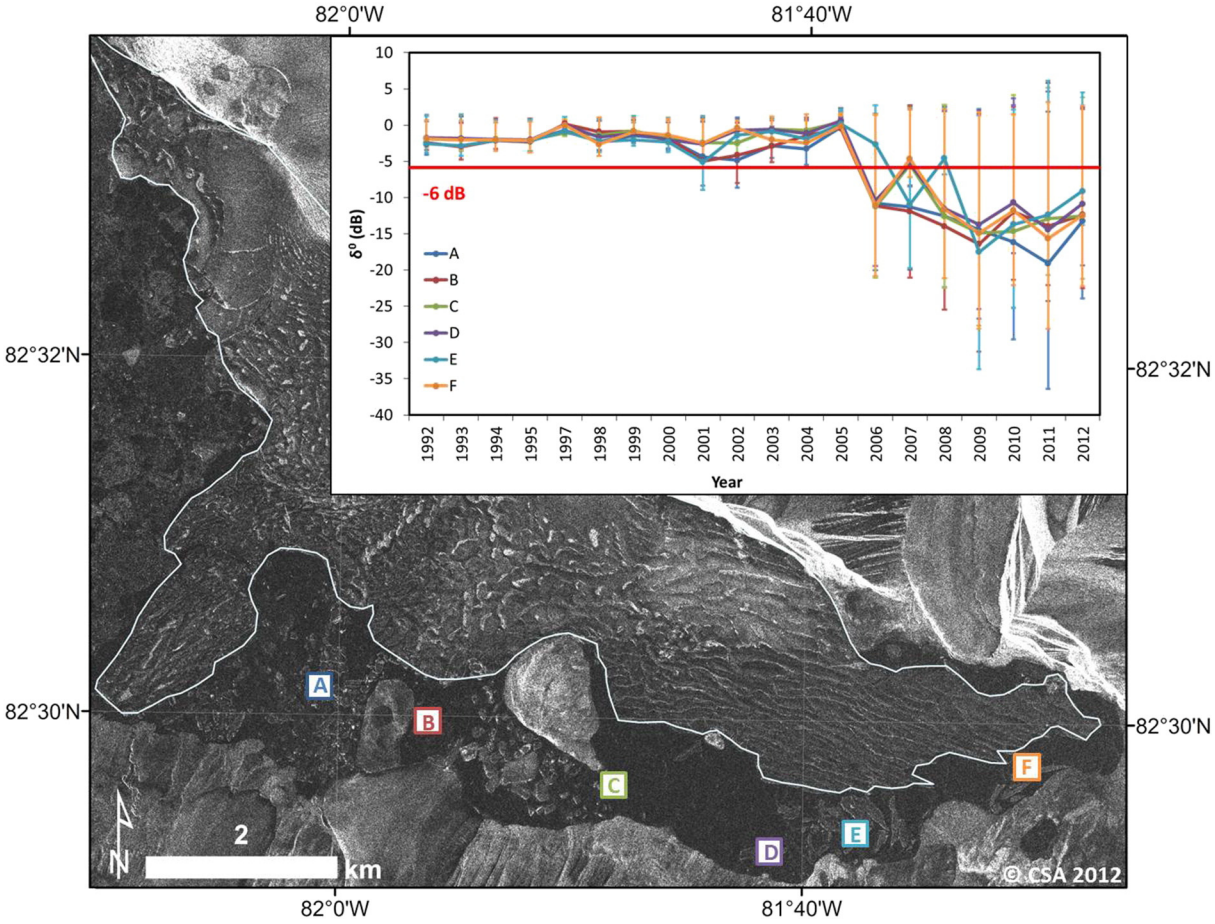

Fig. 4. The six sites selected for sub-regional backscatter analysis within Petersen Bay, overlaid on an Ultrafine Wide Radarsat-2 HH scene (Feb. 3, 2012). Inset: mean sigma nought value extracted from the six sites, +/− one standard deviation. The red line denotes the −6 dB threshold associated with the presence of an ice-dammed lake. (For interpretation of the references to color in this figure legend, the reader is referred to the web version of this article.)

categorized as perennial freshwater ice according to our classification method. This implies that an ice-dammed lake was present in this area, extending to the eastern and northeastern coast over this period (Fig. 5b). For these years, the lake area ranged from a minimum of 3.7 km^2 in 2001 to a maximum of 5.6 km^2 in 1998 and 2000 (Fig. 6).

By March 2005, however, there was a marked drop in the lake area to 2.0 km^2 from 5.2 km^2 in 2004. This was followed by a further drop in area from 2005 to 2006, when the lake area decreased to 1.5 km^2 (Figs. 5c–d, 6). From 2006 to 2012 the area of backscatter above the −6 dB threshold remained minimal, ranging from 0.02 km^2 to 0.8 km^2 (Figs. 5e–g, 6 and 7).

4.2. Spatial analysis of backscatter

Until 2005, all study sites shown in Fig. 4 had mean backscatter values above the −6 dB threshold, but after this time the backscatter was much more variable across the lake. Between 2005 and 2006, sites A, B, C, D and F all demonstrated a large decrease in mean backscatter, by 10.5–11.8 dB (Fig. 4 inset). Site E, however, maintained a mean backscatter of −2.7 dB during this time, well above the −6 dB threshold. Visual assessment of a standard beam Radarsat-1 HH scene (January 14, 2006) shows an area of high backscatter in the region of site E, with an area of ~0.7 km^2 ('Ephemeral' region in Fig. 5d). By January 26, 2007, Radarsat-1 imagery showed a decrease in backscatter at site E to ~−11.0 dB (Fig. 4 inset). However, sites C, D and F had an increase (to −5.5, −5.3 and −4.7 dB respectively) in their backscatter above the lake ice threshold, while all other sites maintained values below −11.0 dB. In 2008, site E became the only region with high backscatter returns (~ −4.6 dB), while all other sites remained low (Figs. 4 inset and 5e).

4.3. Validation of ice type classification using ice cores

Ice cores collected from four sites along the southern coast of Petersen Bay had highly variable bulk salinity values that were inconsistent with freshwater lake ice cover in 2009, 2011 and 2012 (Fig. 8). Ice cores extracted in 2009 from sites 1, 2 and 3 (Fig. 1b) contained saline ice at 35 to 57 cm depth (Fig. 8a). The ice core collected at site 1 in 2011 showed a slight increase in salinity with depth, although the salinity remained <1 psu throughout the core profile (Fig. 8b). The occurrence of vertical veins at the top of the core is likely due to the presence of brine inclusions (Wadhams, 2000).

The ice cores collected from the four sites in late winter 2012 displayed very little variability in thickness and salinity (Fig. 8c). Upper portions of all cores had salinities of <1 psu, which transitioned to slightly higher salinities (~2 psu) towards the base of the core. All of the cores were also similar in terms of their stratigraphy, with the near surface characterized by cloudy ice with large rounded bubbles. These surface characteristics are consistent with snow ice (i.e. white ice), which is formed when enough snow falls on the ice cover during formation to depress it below the water surface (Adams & Roulet, 1980; Duguay, Pultz, Lafleur, & Drai, 2002). This snow ice layer was underlain by a thicker layer of clear ice with small bubble trains throughout. This layer eventually transitioned into increasingly cloudier ice

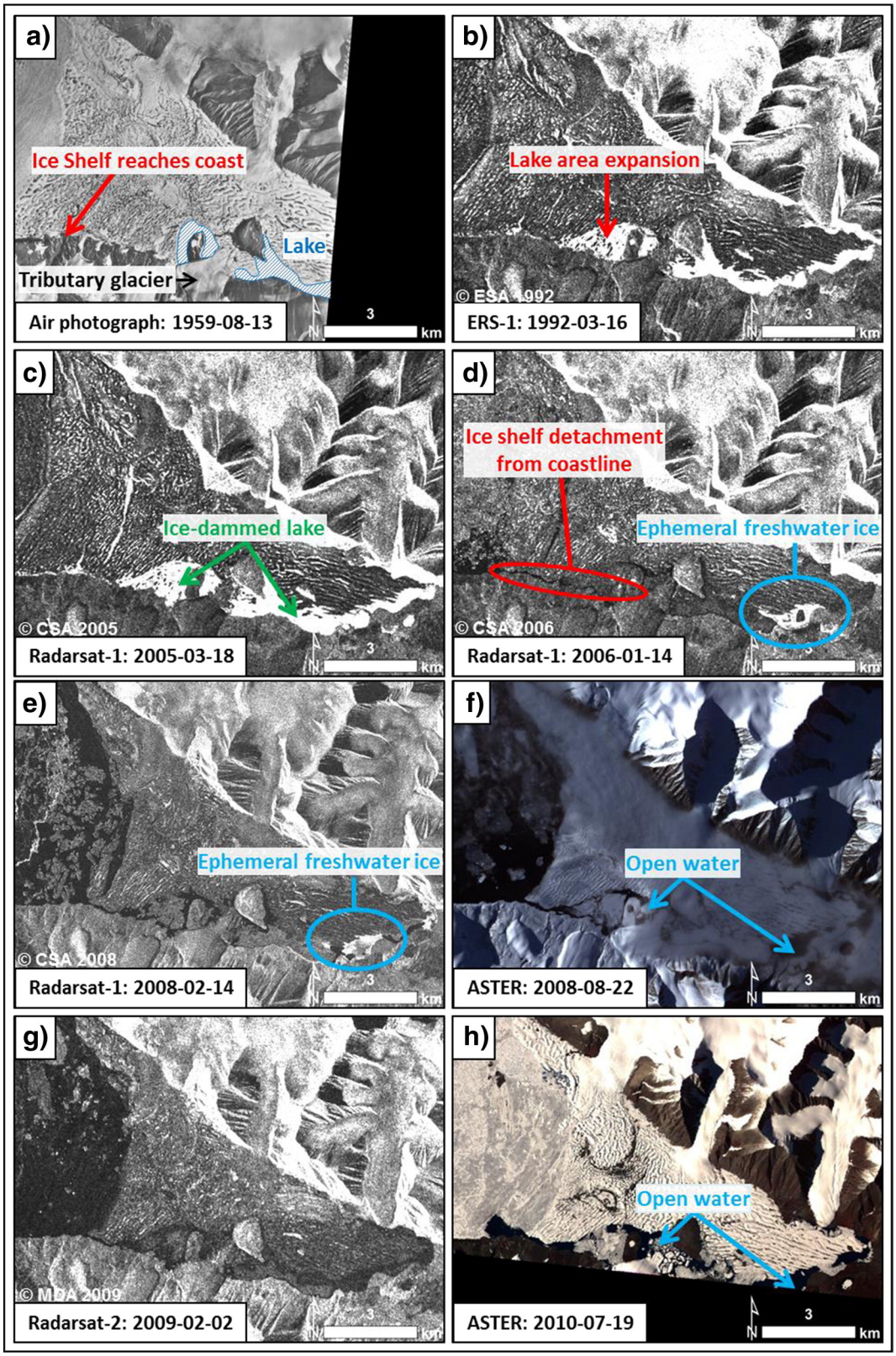

Fig. 5. Aerial photography and satellite imagery showing: (a) lake extent in 1959; (b) expansion of the ice-dammed lake to the west of the island in March 1992; (c) evidence for the ice-dammed lake as bright backscatter across the bay, adjacent to the Petersen Ice Shelf, in March 2005; (d) loss of the ice-dammed lake, but remaining ephemeral freshwater regions identified by higher backscatter in January 2006; (e) ephemeral freshwater region in February 2008; (f) open water across the Petersen Bay lake area in August 2008; (g) low backscatter across entire southern coast in February 2009 indicates complete loss of any ice-dammed lake; (h) open water across the Petersen Bay lake area in July 2010. Note that the high backscatter artifact visible at the base of the mountains along the north side of the ice shelf (in b, c, and d) is due to layover, which occurs when the radar returns from the top of a slope before the bottom of the slope (Campbell, 2002).

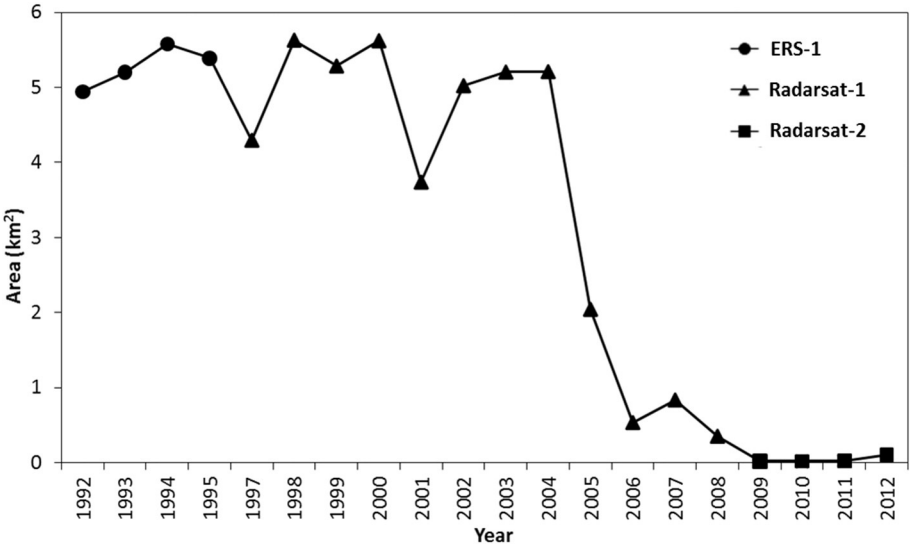

Fig. 6. Changes in freshwater ice and lake area determined through backscatter threshold classification from 1992 to 2012.

with elongated bubbles, followed by the basal ice characterized by cloudy ice with small rounded bubbles.

The above descriptions confirm the presence of saline ice along the southern coast of Petersen Bay since 2009 and, by inference, liquid brine in at least the base of the cores. It is this characteristic that is important to connect with the transition from high to low backscatter observed in the SAR imagery. Stable isotope data would be required to unambiguously differentiate between fresh, brackish and marine ice in the cores (Jeffries, Krouse, Sackinger, & Serson, 1989), but having this information wouldn't change the interpretations here.

4.4. Validation of ice type as an indicator of an ice-dammed lake

To validate the effectiveness of backscatter analysis in identifying lake ice vs sea ice and ultimately the hydrography of the underlying water column, CTD profiles from site 1 (Fig. 1b) were compared with backscatter analysis at site E (Fig. 4), which are co-located in the southeast side of the bay. The salinity ranges were defined by 0–0.49 psu for fresh, 0.5–17 for brackish and >17 psu for seawater (U.S. Naval Oceanographic Office, 1966). In May 2008, a CTD profile detected fresh and brackish water down to 5.6 m with a maximum salinity of 8.63 psu,

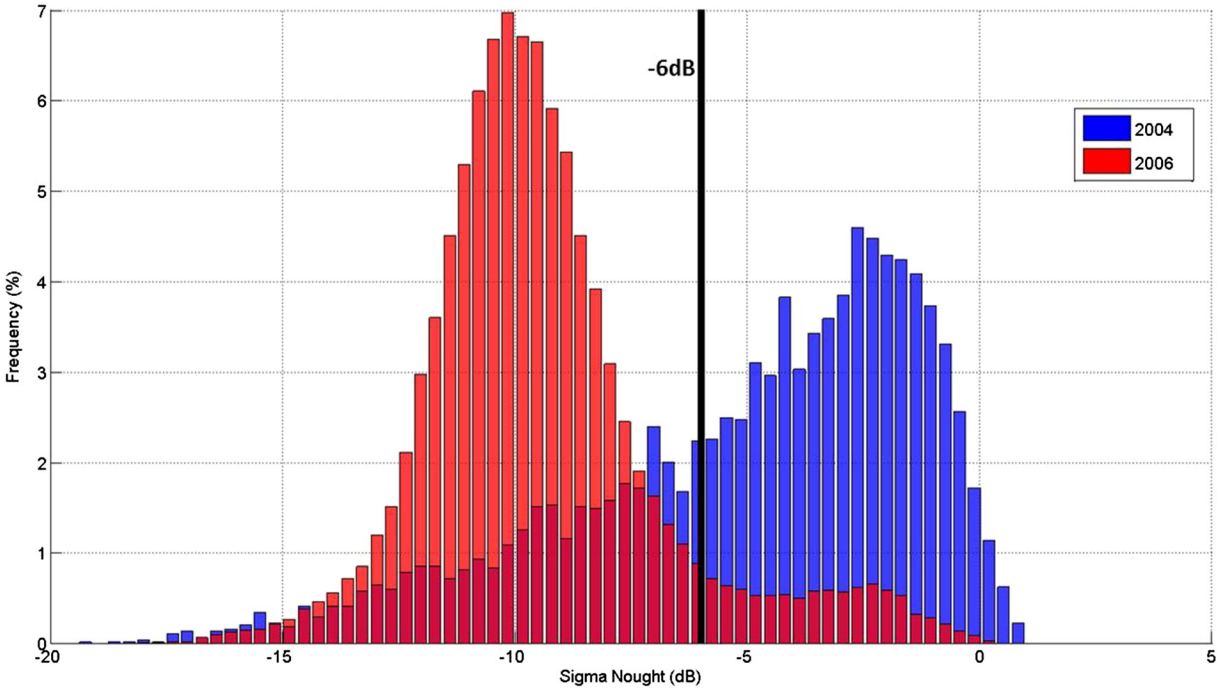

Fig. 7. Histogram indicating the change in distribution of backscatter across Petersen Bay before and after the first major break up of the Petersen Ice Shelf, on December 12, 2004 (red) and January 14, 2006 (blue), respectively. In 2004 the predominantly >−6.0 dB backscatter is indicative of lake ice, while the <−6.0 dB backscatter in 2006 is indicative of sea ice. (For interpretation of the references to color in this figure legend, the reader is referred to the web version of this article.)

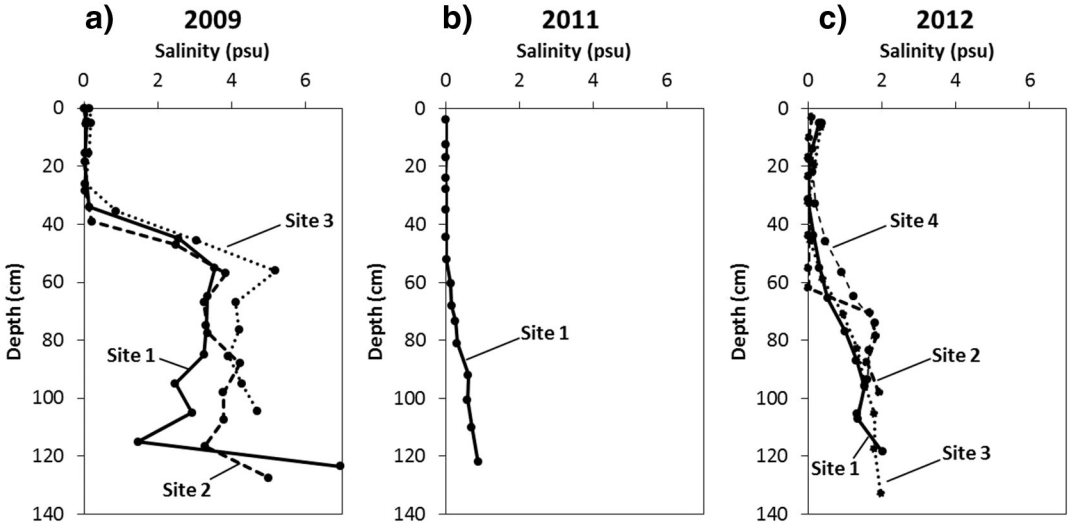

Fig. 8. Ice core salinity measurements from Petersen Bay in: (a) May 2009; (b) May 2011; (c) May 2012. All ice cores penetrated the full ice thickness (see Fig. 1 for location of sites).

while site E had a mean sigma nought value of −4.6 dB (in February 2008) (Fig. 4 and 9a). This high backscatter and low salinity water profile is consistent with the presence of an ice-dammed lake in this location. By 2009, when the CTD profile was saline throughout the water column (~30 psu), the mean backscatter of ice at this site decreased to −17.5 dB, well below the −6 dB threshold for the presence of lake ice (Fig. 9a). The ice core collected from site 1 in 2009 confirmed the presence of sea ice due to high salinity levels in the lower 2/3 of the core, providing further evidence that an ice-dammed lake was absent at that time. Based on this field validation, it is reasonable to assume that backscatter values > −6 dB are indicative of lake ice in Petersen Bay.

In 2011 the CTD profile revealed a thin (<2.4 m) layer of brackish water (8.9 to 16.8 psu) (Fig. 9a). However, in 2012 this brackish layer was replaced by increasingly saline values from 22.7 psu at the surface, transitioning to ~28 psu by 4.8 m depth (Fig. 9a).

4.5. Open water events

Based on the persistence of the ice-dammed lake, and the stability of the glacier tongue flowing towards the ice shelf (on the southern coastline) observed in the air photos, Radarsat-1 and ASTER imagery, it is likely that minimal to no open water occurred from 1959 to 2005 (Fig. 5a–c). There is limited recent cloud-free optical satellite imagery with coverage over Petersen Bay available in July/August (when open water could occur), although an ASTER image from August 22, 2008 clearly shows extensive open water throughout the southern portion of Petersen Bay and along the front of Petersen Ice Shelf. Open water throughout the southern portion of the bay was again observed in ASTER imagery acquired on July 19, 2010 and July 15, 2012. The gradual break-up and disintegration of the glacier tongue to the south is visible throughout the scenes, and also suggests that open water did not occur

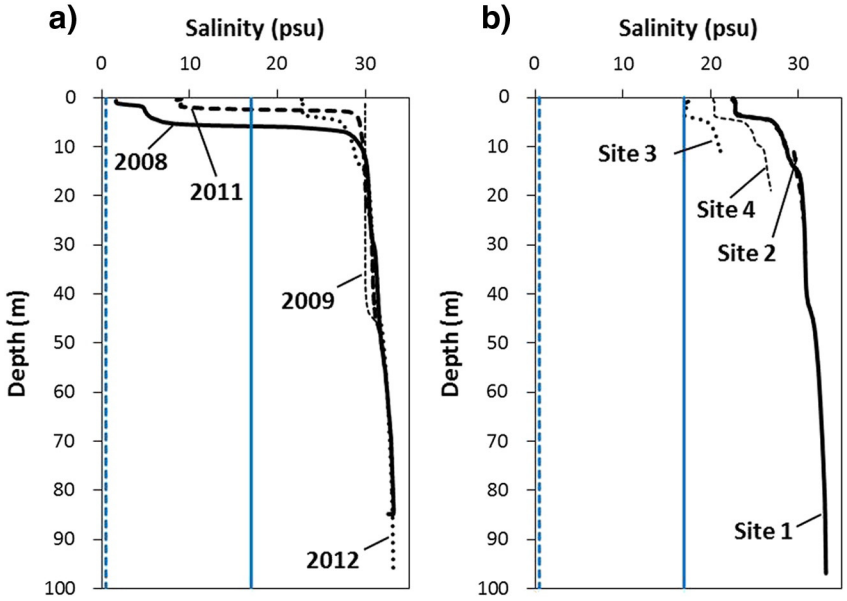

Fig. 9. CTD profiles showing the variation in salinity with depth in Petersen Bay between: (a) April 2008, May 2009, May 2011 and May 2012 at site 1 (ephemeral lake region) and; (b) All sites (1, 2, 3 and 4 in Fig. 1) in May 2012. The dotted blue line represents the transition from fresh to brackish water (0.5 psu), while the solid blue line represents the transition from brackish water to seawater (17 psu) (U.S. Naval Oceanographic Office, 1966). (For interpretation of the references to color in this figure legend, the reader is referred to the web version of this article.)

extensively prior to the 2000s, when the glacier tongue was connected to the ice shelf and remained intact from 1959 to ~2008.

5. Discussion

Based on the high backscatter values observed in early SAR imagery, and the stability of the Petersen Ice Shelf and adjacent MLSI prior to 2005, it is likely that an ice-dammed lake existed in Petersen Bay from 1959 to 2005. In 1959, aerial photography indicates that the Petersen Ice Shelf occupied the majority of Petersen Bay, including the southern coast, with the exception of an area in the southeast region of the bay which may have been covered by lake ice. As the ice shelf began to decrease in area, at its front and along its southern margin, from the 1950s onward (White et al., 2015), the lake area expanded to occupy the areas once filled by the ice shelf. In 1992, the ice-dammed lake had an area of 4.9 km^2. From 1992 to 2004, the lake area ranged from 3.7 to 5.6 km^2, but it was always present. Based on backscatter analysis by sub-region, strong returns (>−6 dB) indicative of lake ice were generally consistent across the bay until 2005.

In summer 2005, a significant calving from the front of the Petersen Ice Shelf reduced its area by 8.07 km^2, equivalent to 16% of its area at that time (White et al., 2015). This loss, along with the complete calving of the nearby Ayles Ice Shelf in 2005, occurred following the break-up of MLSI that provided a protective buffer along the seaward edge of the ice shelves (Copland et al., 2007; Pope, Copland, & Mueller, 2012; White et al., 2015). Copland et al. (2007) also associated the 2005 break-ups of the Ayles and Petersen ice shelves with exceptional climatic conditions that year, including an early onset of the melt season, the second highest number of positive degree days since 1948, particularly warm air temperatures in the month prior to the break ups (2.1 °C above the 1948–2006 average), and strong offshore and along shore winds (up to 90 km h^{-1}). A study focusing specifically on the Petersen Ice Shelf by White et al. (2015) reported major calving events from the ice shelf in 2005, 2008, 2011 and 2012 and attributed these events to the loss of MLSI, fast ice and open water, record high mean summer temperatures, and to the presence of pre-existing fractures and ice shelf thinning. After the calving event in 2005, the Petersen Ice Shelf no longer provided a viable dam and the freshwater lake drained, likely along the southern coast of the bay where the ice shelf became detached from the coastline (Figs. 5d and 10). This detachment was first detected in Radarsat-1 imagery from August 2005, when a meandering channel became apparent between the ice shelf and the southern coastline, providing a conduit for freshwater to escape. This type of drainage is reminiscent of the meandering channel that formed along the center of the Ward Hunt Ice Shelf in 2002, which provided a conduit for the drainage of the epishelf lake from Disraeli Fiord (Mueller et al., 2003). Based on the likelihood that the Petersen Bay ice-dammed lake contained a rare ecosystem similar to the epishelf lakes at the Milne and Ward Hunt ice shelves (Van Hove et al., 2001; Veillette et al., 2011), the loss of this habitat would have resulted from the drainage.

After August 2005, an ephemeral freshwater region reformed in the southeast part of the lake, at the edge of an alluvial fan (Fig. 10, inset) where a major source of inflow can be observed in optical satellite imagery and in the field. The presence of this freshwater region was verified by field measurements in winter 2008, but did not appear to be present between 2009 and 2012 when open water conditions began to occur throughout the summer months. Open water in the lake area would have facilitated wind mixing and breakdown of the stratification in the water column. This is supported by the results from a CTD profile from the ephemeral lake region in May 2009 which showed a salinity of ~30 psu from the surface to the bottom of the water column (Fig. 9a). The loss of the ephemeral lake was likely influenced by open water conditions in summer 2008 when a large fissure, once again, formed along the southern coast between the ice shelf and the land. Ice core analysis in 2009 confirmed the presence of sea ice in three different areas of the former ice-dammed lake area (Fig. 8a). The transition from ephemeral freshwater regions to marine water and sea ice in Petersen Bay followed the second major break up of the Petersen Ice Shelf (−8.99 km^2) in summer 2008 and a large scale open water event in the former lake area (White et al., 2015). The break-up of the

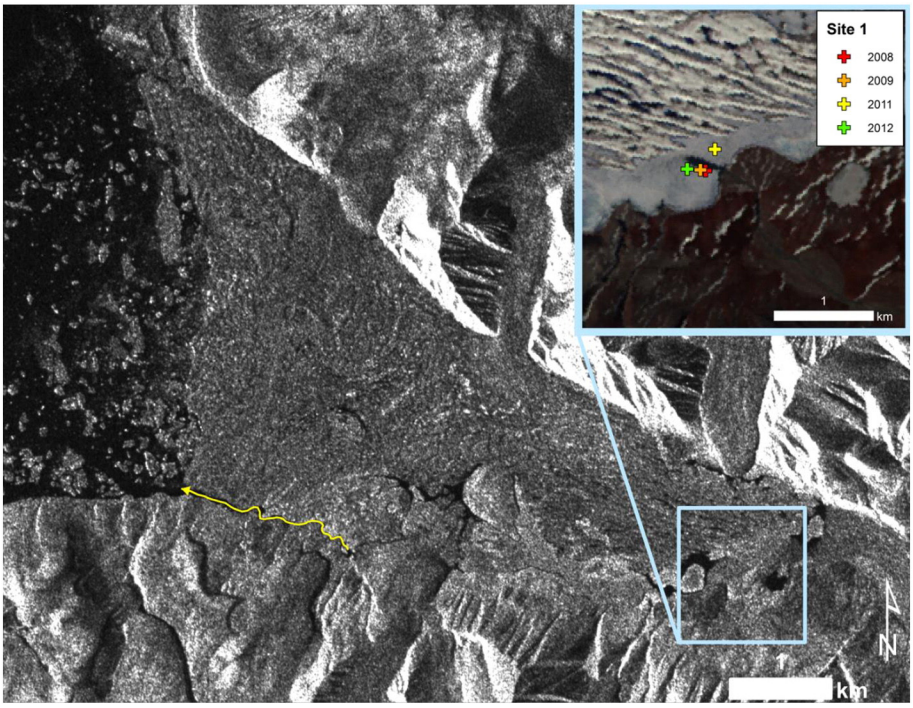

Fig. 10. Radarsat-1 scene from August 18, 2005, showing the meandering drainage channel (yellow arrow) along the southern edge of Petersen Ice Shelf. Inset: ASTER L1B satellite image (July 14, 2009) showing the measurement locations at site 1, the pathway of major terrestrial freshwater inflow and an alluvial fan along the coast of the lake area. (For interpretation of the references to color in this figure legend, the reader is referred to the web version of this article.)

ice shelf also coincided with the second major loss of MLSI from Yelverton Bay in summer 2008 (Pope et al., 2012).

Since 2009, remote sensing, ice core and CTD data suggest that the entire area formerly occupied by the ice-dammed lake has become a marine environment with freshwater input provided by seasonal runoff. The vast open water event that occurred in summer 2010 also supports this interpretation (Fig. 5h). The ice cores extracted from several sites in May 2012 indicated a salinity profile consistent sea ice (Fig. 8c). The CTD profiles collected in May 2012 detected a brackish layer (reaching the top of the halocline by ~0.7 to ~1.3 m depth) across the lake area, which suggests that freshwater inflow may have become impounded by relatively thick sea ice at the outlet of the bay between the coast and the remaining ice shelf (Fig. 9b). This freshwater may have come from terrestrial snow and ice-melt runoff, surface melt of the ice shelf or may be associated with sea ice melt from the previous summer (Gibson & Andersen, 2002). Although this thin brackish layer exists, it is not fresh enough to be considered an ice-dammed lake.

6. Conclusions

Through the use of SAR imagery, CTD profiles and ice cores we have validated the ability to detect the presence of an ice-dammed lake via delineation of perennial lake ice from other ice types. This technique was used to infer the presence of an ice-dammed lake in Petersen Bay from 1992 to 2005 and to document the environmental change that occurred following the ice shelf break up. As of May 2012, Petersen Bay had a multiyear sea ice cover with a mean thickness of 0.86 m. The water below this ice cover was characterized by ~3 m of brackish water underlain by marine water. The bay has experienced unusually long periods of open water in most summers since 2005, reflecting a new ice regime in this area. It is likely that any chance of lake regeneration is impeded by these open water events and the lack of a thick ice plug between the ice shelf and the coast. Under the present climate regime it is unlikely that Petersen Ice Shelf will regrow, making it unlikely that the ice-dammed lake that was probably present for >40 years, and possibly much longer, will form again in the foreseeable future. Even if the Petersen Ice Shelf stopped calving, mass balance estimates by White et al. (2015) indicate that thinning rates (28.45 Mt a^{-1}) far outweigh the contributions of mass via glacier inflow (1.19–5.65 Mt a^{-1}) and snowfall. Ice-dammed lakes and epishelf lakes have the potential to facilitate basal accumulation on ice shelves via freshwater underflow, meaning that the regrowth of the ice shelf as a viable dam for the lake is hindered by the loss of the lake itself (Jeffries, 1992a). However, should this feature return, it will be possible to use future SAR imagery and the technique presented here to detect this environmental change.

Acknowledgments

We would like to thank the Canada Foundation for Innovation, Ontario Research Fund, National Sciences and Engineering Research Council of Canada, Garfield Weston Foundation, Royal Canadian Geographic Society, Polar Continental Shelf Program, Northern Scientific Training Program, ArcticNet, Carleton University and University of Ottawa for financial and logistical support. We would also like to thank Andrew Hamilton (University of British Columbia) and Miriam Richer-McCallum (Carleton University) for assistance in the field. RADARSAT-2 data were provided under the SOAR-E program (project # 5054) by MacDonald, Dettwiler and Associates (MDA) under the RADARSAT-2 Government Data Allocation administered by the Canadian Space Agency. ERS-1 and RADARSAT-1 data were provided by the Alaska Satellite Facility.

References

Adams, W.P., & Roulet, N.T. (1980). Illustration of the roles of snow in the evolution of the winter cover of a lake. *Arctic*, *33*(1), 100–118.

AMAP (2011). *Snow, water, ice and permafrost in the Arctic (SWIPA): Climate change and the cryosphere*. Oslo, Norway: Arctic Monitoring and Assessment Programme (AMAP) (538 pp).

Campbell, J.B. (2002). *Introduction to remote sensing* (3rd ed.). New York: Guilford.

Comiso, J.C., Parkinson, C.L., Gersten, R., & Stock, L. (2008). Accelerated decline in the Arctic sea ice cover. *Geophysical Research Letters*, *35*(L01703)http://dx.doi.org/10.1029/2007GL031972.

Copland, L., Mueller, D.R., & Weir, L. (2007). Rapid loss of the Ayles Ice Shelf, Ellesmere Island, Canada. *Geophysical Research Letters*, *34*(L21501)http://dx.doi.org/10.1029/2007GL031809.

Crary, A.P. (1960). Arctic ice islands and ice shelf studies, part II. *Arctic*, *13*(1), 32–50.

Duguay, C.R., Pultz, T.J., Lafleur, P.M., & Drai, D. (2002). RADARSAT backscatter characteristics of ice growing on shallow sub-Arctic lakes, Churchill, Manitoba, Canada. *Hydrological Processes*, *16*(8), 1631–1644http://dx.doi.org/10.1002/hyp.1026.

England, J.H., Lakeman, T.R., Lemmen, D.S., Bednarski, J.M., Stewart, T.G., & Evans, D.J.A. (2008). A millennial-scale record of Arctic Ocean sea ice variability and the demise of the Ellesmere Island ice shelves. *Geophysical Research Letters*, *35*(19)http://dx.doi.org/10.1029/2008GL034470.

Fofonoff, P., & Millard, R.C., Jr. (1983). Algorithms for computation of fundamental properties of seawater. *UNESCO Technical Papers in Marine Science*, *44* (58 pp).

Gardner, A.S., Moholdt, G., Wouters, B., Wolken, G.J., Burgess, D.O., Sharp, M.J., et al. (2011). Sharply increased mass loss from glaciers and ice caps in the Canadian Arctic Archipelago. *Nature*, *473*(7347), 357–360.

Gibson, H.A.E., & Andersen, D.T. (2002). Physical structure of epishelf lakes of the southern Bunger Hills, East Antarctica. *Antarctic Science*, *14*(3), 253–261http://dx.doi.org/10.1017/S095410200200010X.

Heywood, R.B. (1977). A limnological survey of the Ablation Point area, Alexander Island, Antarctica. *Philosophical Transactions of the Royal Society B*, *279*(963), 39–54.

Jeffries, M.O. (1992a). Arctic ice shelves and ice islands: origin, growth and disintegration, physical characteristics, structural-stratigraphic variability, and dynamics. *Reviews of Geophysics*, *30*(3), 245–267http://dx.doi.org/10.1029/92RG00956.

Jeffries, M.O. (1992b). The source and calving of ice island ARLIS-II. *Polar Record*, *28*(165), 137–144http://dx.doi.org/10.1017/S0032247400013437.

Jeffries, M.O. (2002). Ellesmere island ice shelves and ice islands. In R.S. Williams, & J.G. Ferrigno (Eds.), *Satellite image atlas of glaciers of the world: Glaciers of North America. U.S. Geological Survey Professional Paper, 1386-J-1*. (pp. J147–J164).

Jeffries, M.O., Krouse, H.R., Sackinger, W.M., & Serson, H.V. (1989). Stable-isotope ($^{18}O/^{16}O$) tracing of fresh, brackish, and sea ice in multi-year land-fast sea ice, Ellesmere Island, Canada. *Journal of Glaciology*, *35*(119), 9–16http://dx.doi.org/10.3189/002214389793701473.

Jeffries, M.O., Morris, K., & Kozlenko, N. (2005). Ice characteristics and processes, and remote sensing of frozen rivers and lakes, p. 63–90. In C.R. Duguay, & A. Pietroniero (Eds.), *Remote sensing in northern hydrology*. American Geophysical Union.

Jeffries, M.O., Morris, K., Weeks, W.F., & Wakabayashi, H. (1994). Structural and stratigraphic features and ERS 1 synthetic aperture radar backscatter characteristics of ice growing on shallow lakes in NW Alaska, winter 1991–1992. *Journal of Geophysical Research*, *99*(C11), 22459–22471http://dx.doi.org/10.1029/94JC01479.

Jeffries, M.O., & Sackinger, W.M. (1990). Airborne SAR characteristics of arctic ice shelves and multiyear landfast sea ice, and the detection of massive ice calvings and ice islands. *Geoscience and remote sensing symposium, IGARSS'89. 12th Canadian Symposium on Remote Sensing*.

Johnston, M.E., & Timco, G.W. (2008). *Understanding and identifying old ice in summer*. Ottawa: Canadian Hydraulics Centre, National Research Council (236 pp).

Jungblut, A.D., Mueller, D.R., & Vincent, W.F. (2015). Arctic ice shelf ecosystems. In L. Copland, & D.R. Mueller (Eds.), *Arctic ice shelves and ice islands*. Dordrecht: Springer SBM (in press).

Kaufman, D.S., Schneider, D.P., McKay, N.P., Ammann, C.M., Bradley, R.S., Briffa, K.R., et al. (2009). Recent warming reverses long-term Arctic cooling. *Science*, *325*(1236), 1236–1239http://dx.doi.org/10.1126/science.1173983.

Keys, J.E. (1977). *Water regime of ice-covered fiords and lakes*. McGill University.

Kwok, R., & Rothrock, D.A. (2009). Decline in Arctic sea ice thickness from submarine and ICESat records: 1958–2008. *Geophysical Research Letters*, *36*(L15501)http://dx.doi.org/10.1029/2009GL039035.

Laybourne-Parry, J., Quayle, W.C., Henshaw, T., Ruddell, A., & Marchants, H.J. (2001). Life on the edge: The plankton and chemistry of Beaver Lake, an ultra-oliographic epishelf lake, Antarctica. *Freshwater Biology*, *46*, 1205–1217http://dx.doi.org/10.1046/j.1365-2427.2001.00741.x.

Lillesand, T.M., Kiefer, R.W., & Chipman, J.W. (2008). *Remote sensing and image interpretation* (6th ed.). USA: John Wiley and Sons Inc.

Maslanik, J., Stroeve, J., Fowler, C., & Emery, W. (2011). Distribution and trends in Arctic sea ice age through spring 2011. *Geophysical Research Letters*, *38*(L13502)http://dx.doi.org/10.1029/2011GL047735.

Mueller, D.R., Crawford, A., Copland, L., & Van Wychen, W. (2013). *Ice island and iceberg fluxes from Canadian High Arctic sources*. Report to the Northern Transportation Assessment Initiative, Innovation Policy Branch, Transport Canada, Ottawa, ON, Canada, 23.

Mueller, D.R., Vincent, W.F., & Jeffries, M.O. (2003). Break-up of the largest Arctic ice shelf and associated loss of an epishelf lake. *Geophysical Research Letters*, *30*(20)http://dx.doi.org/10.1029/2003GL017931.

Mueller, D.R., Vincent, W.F., & Jeffries, M.O. (2006). Environmental gradients, fragmented habitats, and microbiota of a northern ice shelf cryoecosystem, Ellesmere Island, Canada. *Arctic, Antarctic, and Alpine Research*, *38*(4), 593–607http://dx.doi.org/10.1657/1523-0430(2006)38[593:EGFHAM]2.0.CO;2.

Onstott, R.G., & Shuchman, R.A. (2004). Chapter 3. SAR measurements of sea ice. In C.R. Jackson, & J.R. Apel (Eds.), *Synthetic aperture radar marine user's manual*. Washington, DC: National Oceanic and Atmospheric Administration (464 pp).

Pope, S., Copland, L., & Mueller, D. (2012). Loss of multiyear landfast sea ice from Yelverton Bay, Ellesmere Island, Nunavut, Canada. *Arctic, Antarctic, and Alpine Research*, *44*(2), 210–221http://dx.doi.org/10.1657/1938-4246-44.2.210.

Shepherd, A., Ivins, E.R., Geru, A., Barletta, V.R., Bentley, M.J., Bettadpur, S., et al. (2012). A reconciled estimate of ice-sheet mass balance. *Science*, *338*(6111), 1183–1189.

Stroeve, J., Holland, M.M., Meier, W., Scambos, T., & Serreze, M. (2007). Arctic sea ice decline: Faster than forecast. *Geophysical Research Letters*, *34*(L09501)http://dx.doi.org/10.1029/2007GL029703.

U.S. Naval Oceanographic Office (1966). Glossary of oceanographic terms. In B.B. Baker Jr., W.R. Deebel, & R.D. Geisenderfer (Eds.), (2nd ed.) (Washington, D.C.).

Van Hove, P., Swadling, K.M., Gibson, J.A.E., Belzile, C., & Vincent, W.F. (2001). Farthest north lake and fjord populations of calanoid copepods *Limnocalanus macrurus* and *Drepanopus bungei* in the Canadian high Arctic. *Polar Biology*, *24*(5), 303–307http://dx.doi.org/10.1007/s003000000207.

Veillette, J., Lovejoy, C., Potvin, M., Harding, T., Jungblut, A.D., Antoniades, D., et al. (2011). Milne fiord epishelf lake: A coastal Arctic ecosystem vulnerable to climate change. *Ecoscience*, *18*(3), 304–316http://dx.doi.org/10.2980/18-3-3443.

Veillette, J., Mueller, D.R., Antoniades, D., & Vincent, W.F. (2008). Arctic epishelf lakes as sentinel ecosystems: Past, present and future. *Journal of Geophysical Research*, *113*(G04014)http://dx.doi.org/10.1029/2008JG000730.

Vincent, W.F., Gibson, J.A.E., & Jeffries, M.O. (2001). Ice shelf collapse, climate change, and habitat loss in the Canadian high Arctic. *Polar Record*, *37*(201), 133–142http://dx.doi.org/10.1017/S0032247400026954.

Wadhams, P. (2000). *Ice in the ocean*. Amsterdam: Gordon and Breach Science Publishers.

White, A., Copland, L., Mueller, D., & Van Wychen, W. (2015). Assessment of historical changes (1959–2012) and the causes of recent break-ups of the Petersen Ice Shelf, Nunavut, Canada. *Annals of Glaciology*, *56*(69), 65–76.